Experimental Study of Two-Tone Intermodulation Products in a Communications Modulator

María J. Madero-Ayora, Michel Allegue-Martínez, Carlos Crespo-Cadenas, Javier Reina-Tosina, Javier Navarro-Lázaro

Dpto. de Teoría de la Señal y Comunicaciones

Escuela Superior de Ingenieros, Universidad de Sevilla

Camino de los Descubrimientos, s/n.; 41092 -- Seville, Spain

Phone: +34 95 4487334; Fax: +34 95 4487341; E-mail: mjmadero@us.es

ABSTRACT

This paper presents the experimental nonlinear characterization of a quadrature modulator following a two-tone test approach. The observed intermodulation products show different slopes with respect to the desired carrier level that can be predicted by a simple model. Measurements for two-tone tests versus carrier level and tone spacing are discussed.

INDEX TERMS

Communications quadrature modulator, intermodulation products, nonlinear distortion, two-tone test.

I. INTRODUCTION

Microwave or RF waveform generators, and specially quadrature modulators, constitute a fundamental element in any wireless communications system. Signals generated by them are injected into diverse types of devices, including power amplifiers (PAs), mixers, filters, passive networks, etc. In case an appropriate characterization of the modulator is non-existent, distortion behaviors caused by the transmitter itself could be wrongly attributed to other devices, rendering potential linearization techniques applied to them useless.

Despite the important advances achieved in the characterization of PAs and signal predistortion in order to compensate for their nonlinear behavior, quadrature modulators have not been sufficiently studied yet. The ideal linear behavior of these systems is affected by impairments such as carrier leakage, differential gain error between the in-phase (I) and quadrature (Q) signal paths, and error in the 90-degree shift between them, with the subsequent distortion of the modulated signal. When combined with the rest of the communications system, these behaviors produce non-negligible intermodulation (IM) products and a degradation of the Bit Error Rate (BER) [1]-[4].

This paper is aimed at the experimental nonlinear characterization of a communications modulator following a standard approach based on a two-tone test. The outline is as follows: in Section II, some models for quadrature modulators and their limitations are reviewed; in order to evaluate the performance of the adopted model, its predictions are compared in Section III with measurements of two-tone IM products; finally, Section IV presents some conclusions.

II. MODELS FOR QUADRATURE MODULATORS

During the last decades, some linear models for the characterization of the impairments present in quadrature modulators have been proposed. In [1] and [2], different techniques to correct imperfections of modulators such as carrier leakage, differential gain error and phase mismatch error were proposed. In addition to these frequency-independent or static models, a frequency-dependent model and compensation technique was presented in [3]. Despite their different approaches, these works are based on the use of simple linear analytical models for the quadrature modulator that only account for dc offsets and differential gain and quadrature phase errors between the I and Q paths.

An initial verification in the experimental characterization carried out in this work consisted in analyzing the output spectrum obtained for a standard two-tone signal. A commercial Rohde & Schwarz SMIQ02B signal generator with built-in arbitrary waveform facility has been employed. Fig. 1 shows the measured output spectrum of the modulator for two tones centered at $f_c = 915$ MHz with a separation $\Delta f = 2$ MHz and a carrier level of +10 dBm. A considerable amount of IM products with non-negligible levels can be observed in it, at frequencies $f_c \pm n f_m$, where $n \in \mathbb{Z}$. Regardless the impairments considered, the only output spectral components that the linear model for the modulator can explain are those at f_c and $f_c \pm f_m$, i.e., the carrier residue and the possibly asymmetrical tones. This limitation can be overcome by adopting a nonlinear model.

Nonlinear characterization of quadrature modulators has been undertaken in [4]-[6], where nonlinear behaviors are considered, not only due to the output RF amplifier, but also in both I and Q baseband paths attributed to the digital-to-analog converters, reconstruction low-pass filters, mixers, and amplifiers at baseband. By means of these nonlinear models, it is possible to explain all the IM products observed in Fig. 1. A simplified scheme like that shown in Fig. 2 could be assumed for all these nonlinear models, where the input signals are the baseband I and Q channels and the output is the RF bandpass modulated signal, represented in terms of its complex envelope. Diverse alternatives can be considered within this model. In its most general form, it presents different characteristics for the I and Q paths containing a dc offset, which allows the model to account for gain/phase imbalance and carrier leakage. While the output RF amplifier exhibits a bandpass nonlinear characteristic, the I and Q paths constitute baseband nonlinear blocks. On the contrary to [4], where a fixed operation point is used to identify the parameters of the model, in this paper different signal levels will be taken into consideration, like in [5]-[6].

As the objective of this paper is the nonlinear characterization of the modulator, the model shown in Fig. 2 will be adopted with some simplifications based on the results of a preliminary linear characterization of the modulator under study, in which no relevant gain or phase imbalances were found. Thus, as presented in [7], a balanced modulator will be considered in which both I and Q paths are modeled by fifth-order polynomials and no error is assumed in the quadrature shifter:

$$x_{I,Q}(t) = \sum_{r=0}^{R} a_r u_{I,Q}^r(t), \tag{1}$$

with $a_r = 1$ and $\phi = 0^\circ$. Note that the same baseband nonlinearity is being assumed for the relationship between $u_I(t)$ and $\mathrm{x}_I(t)$ than for the relationship between $u_Q(t)$ and $\mathrm{x}_Q(t)$, with a unique set of parameters $a_0, a_1, \cdots, a_5$ since a balanced model is being assumed. The different signal levels will be considered by means of an ideal linear block with variable gain, which differentiates this scheme from the previously proposed. Finally, the following third-order memoryless bandpass nonlinear response will be assumed for the RF amplifier:

$$\tilde{y}(t) = \sum_{k=0}^{K} g_{2k+1} \left|\tilde{x}_l(t)\right|^{2k} \tilde{x}_l(t), \tag{2}$$

where the g_{2k+1} are odd-order coefficients for the relationship between the input complex envelope $\tilde{x}_l(t)$ entering the RF amplifier and the output complex envelope $\tilde{y}(t)$.

III. EXPERIMENTAL RESULTS

The measurement setup used in this study consists of a Rohde & Schwarz SMIQ02B communications signal generator with built-in arbitrary waveform facility and an Agilent E4407B spectrum analyzer, which are controlled by a commercial software installed in a PC via a GPIB interface, as shown in Fig. 3. The SMIQ02B was employed as the quadrature modulator under test whose nonlinear characteristics were evaluated at a center frequency $f_c = 915$ MHz. A two-tone power sweep was performed, for which the two tones were formed by using a double-sideband suppressed-carrier signal modulated by a sinusoidal baseband waveform with frequency f_m, producing two coherent tones with the same level and an exactly constant tone spacing $\Delta f = 2 f_m$. The magnitude of the IM products was measured in the spectrum analyzer. It should be mentioned that, despite their being a standard method for PAs, two-tone tests are a quite novel approach for the nonlinear modeling of quadrature modulators [5].

Firstly, the tone spacing was fixed at $\Delta f = 2$ MHz. The measured output power levels of the distortion components at $f_c \pm n f_m$, with $n = 0,1,\cdots,3$, are depicted with marks in Figs. 4 and 5 as a function of the carrier power. It is important to note that the resolution bandwidth and reference level were properly selected for each measured point so that the IM products could be clearly distinguished from the noise floor of the instrument. Different slopes can be experimentally observed in these measurements. The fundamental tones, the carrier residue and the second-order IM products (IM2) present a 1dB/dB slope for virtually the whole range of power levels available in the generator, while the third-order IM products (IM3) exhibit both 1dB/dB and 3dB/dB slopes, indicating a nonlinear operation zone of the RF amplifier for large values of the input level.

The parameters involved in the balanced nonlinear model have been estimated in the least square error sense, and a simulation of the behavior of the model for a two-tone power sweep is depicted in Figs. 4 and 5 with a dashed line. As it can be observed, the simulated power sweep presents an appropriate agreement with measurements. Despite its simplicity, the adopted nonlinear model is able to explain the different experimental slopes.

Two-tone signals were applied with varying tone spacing in order to assess the frequency dependence of the distortion products. Measurements of the resulting IM products are depicted in circles in Figs 6-8 versus both the tone spacing and carrier power. They present non-constant levels with the different tone spacings, which is an indication of the presence of memory effects [8]. The observed variation has been confirmed to be consistent and therefore it cannot be attributed to noise or measurement errors but to a real behavior of the device. However, the prediction of a memoryless model, shown in Figs. 6-8 with a wireframe, does not depend on Δf and it only adjusts the average value of the measured IM levels. Again, the observed change in the slope of IM3 is adequately predicted by the model.

In addition to this, experimental observations suggest that there is a threshold carrier level before which the RF amplifier behaves quasi-linearly and the output nonlinear distortion components, both even- and odd-order, are attributed to the baseband I and Q paths. Above the aforementioned threshold, the odd-order nonlinearities of the RF amplifier prevail and a slope of 3dB/dB is measured for IM3. For a better visualization of these behaviors, the measured level of the upper IM3 has been depicted separately in Fig. 9. Some interesting characteristics in the variations with Δf must be noticed: they occur for carrier power levels for which the IM products are very weak, at least 60 dB below the tones level, and exhibit a 1dB/dB slope. In addition to this, an asymmetry up to ± 15 dB between the upper and the lower IM products (IM_l and IM_u, respectively) is recognizable in some of the measurements, being specially remarkable for IM2 as observed for the black and white circles shown in Fig. 7. These features indicate that the observed memory effects are caused mainly by the nonlinear transfer functions modeling the baseband I and Q paths.

CONCLUSIONS

In this paper, we have presented an experimental nonlinear characterization of a quadrature modulator for which a nonlinear model has been adopted. The model covers the even- and odd-order distortion generated and its level-dependent behavior. Measurements for the device under test with two-tone signals, including both power and tone spacing sweeps, reveal some memory effects mainly attributed to the baseband nonlinearities in the I and Q paths. Although, according to the authors' experience, the observed even-order nonlinear terms and memory effects are weak, trying to explain them is a relevant task because they could introduce errors in behavioral models for the PAs tested with these signal generators.

ACKNOWLEDGMENTS

This work was supported by the Spanish National Board of Scientific and Technological Research (CICYT) under Project TEC2008-06259/TEC, and by the Regional Government of Andalusia (CICE) under Grant P07-TIC-02649. The work of Mr. Allegue was supported by the Spanish Ministry of Foreign Affairs and Cooperation and the Spanish Agency of International Cooperation for Development.

REFERENCES

[1] M. Faulkner, T. Mattson, and W. Yates, Automatic adjustment of quadrature modulators, Electronics Letters, 27 (3), pp. 214-216, Jan. 1991.

[2] J. Cavers and M. Liao, Adaptative compensation for imbalance and offset losses in direct conversion transceivers, IEEE Transactions on Vehicular Technology, 42 (4), pp. 581-588, Nov. 1993.

[3] L. Ding, Z. Ma, D. R. Morgan, M. Zierdt, and G. Zhou, Compensation of frequency-dependent gain/phase imbalance in predistortion linearization systems, IEEE Transactions on Circuits and Systems I: Regular Papers, 55 (2), pp. 378-385, Feb. 2008.

[4] D. Wisell, Identification and measurement of transmitter nonlinearities, in 56th ARFTG Conference Digest-Fall, Boulder, CO, Nov. 2000, 38, pp. 1-6.

[5] KM. E. Gadringer, C. Schubert, and G. Magerl, Characterization and modeling of direct conversion transmitters, in IEEE 38th European Microwave Conference Proceedings, Amsterdam, The Netherlands, Oct. 2008, pp. 745-748.

[6] H. Cao, A. S. Tehrani, C. Fager, T. Eriksson, and H. Zirath, I/Q imbalance compensation using a nonlinear modeling approach, IEEE Transactions on Microwave Theory and Techniques, 57 (3), pp. 513-518, Mar. 2009.

[7] M. J. Madero-Ayora, M. Allegue-Martínez, and C. Crespo-Cadenas, Experimental study of two-tone IM products in a communications modulator, in Proceedings of the 12th International Symposium on Microwave and Optical Technology, New Delhi, India, Dec. 2009, pp. 149-152.

[8] J. K. Vuolevi, T. Rahkonen, and J. P. Manninen, Measurement technique for characterizing memory effects in RF power amplifiers, IEEE Transactions on Microwave Theory and Techniques, 49 (8), pp. 1383-1389, Aug. 2001.

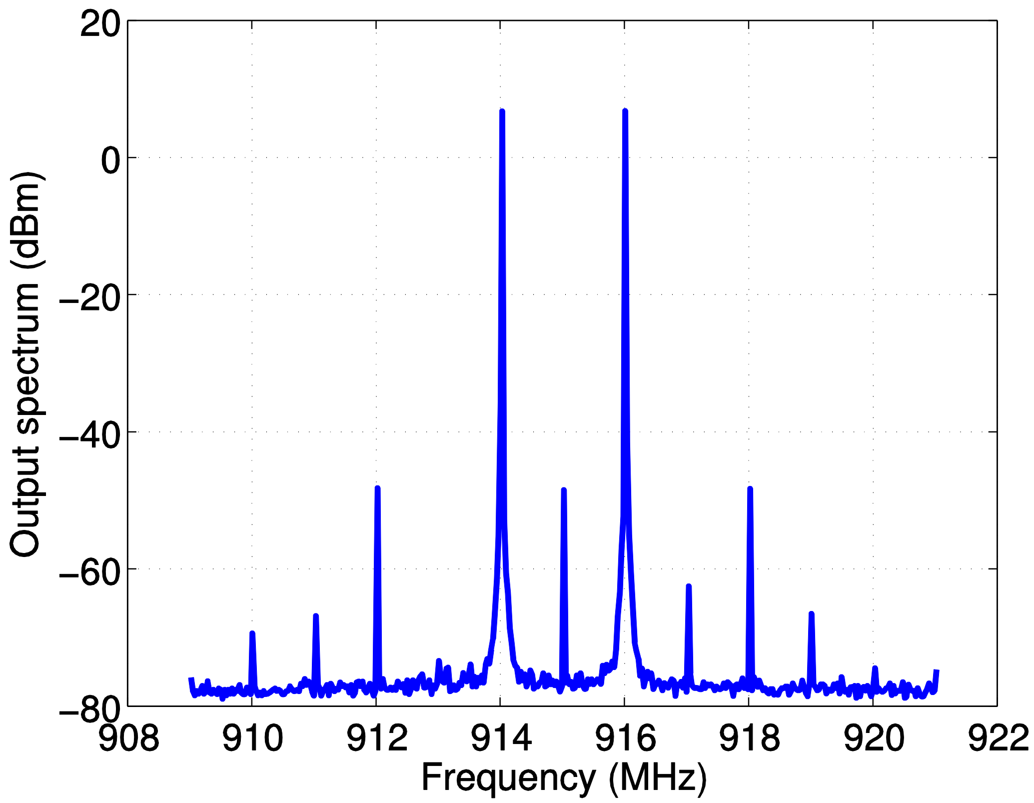

Figure 1: Output spectrum of the quadrature modulator for a two-tone signal with 10 dBm carrier level.

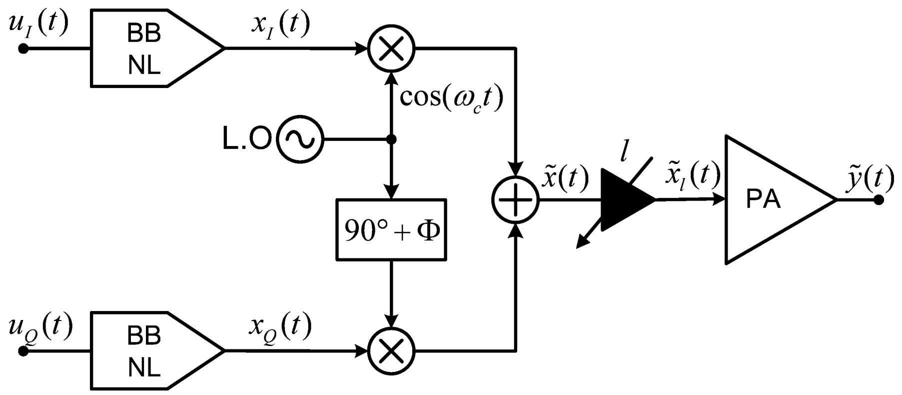

Figure 2: Simplified scheme of the nonlinear model for a quadrature modulator.

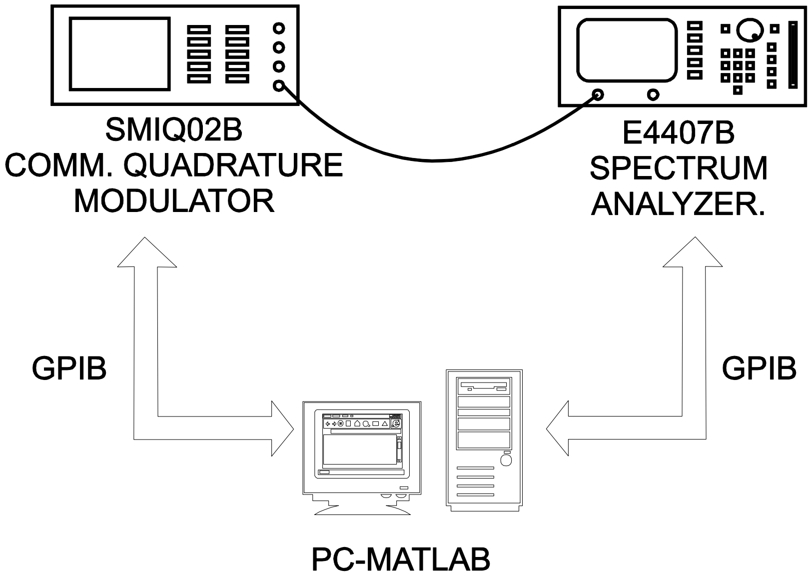

Figure 3: Measurement setup for the experimental nonlinear characterization of the quadrature modulator under test.

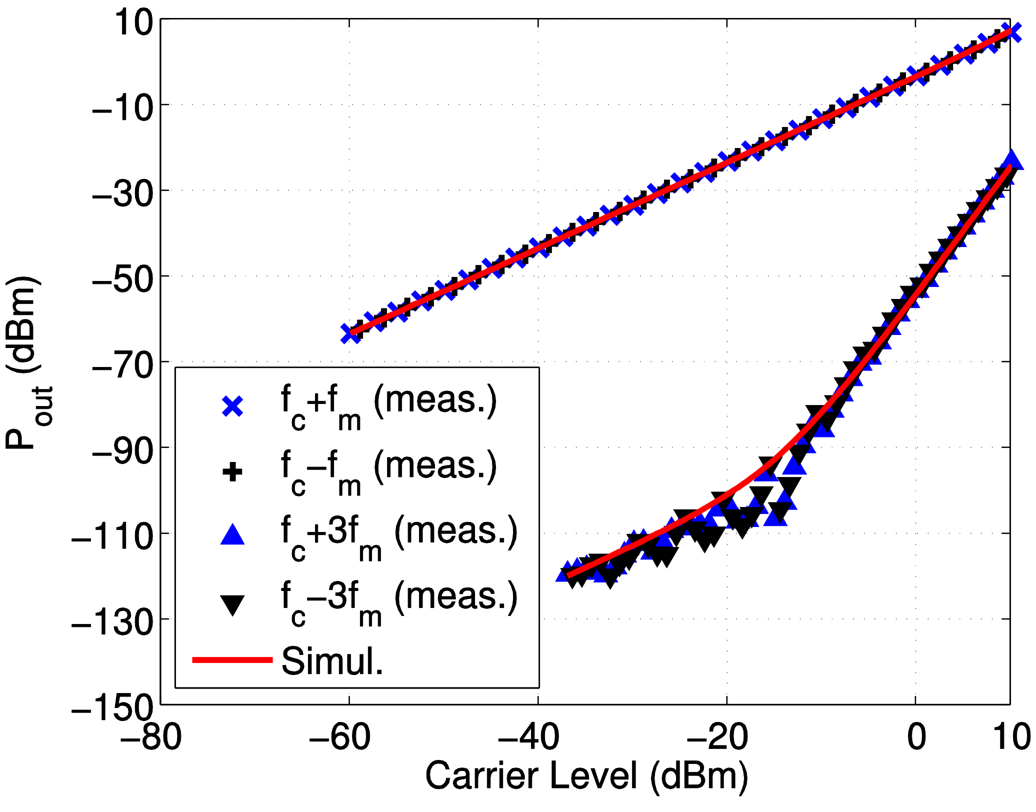

Figure 4: Level of the fundamental tones and IM3 at the output of the modulator versus the carrier power. Measurements (marks) and simulation (dasehd line)

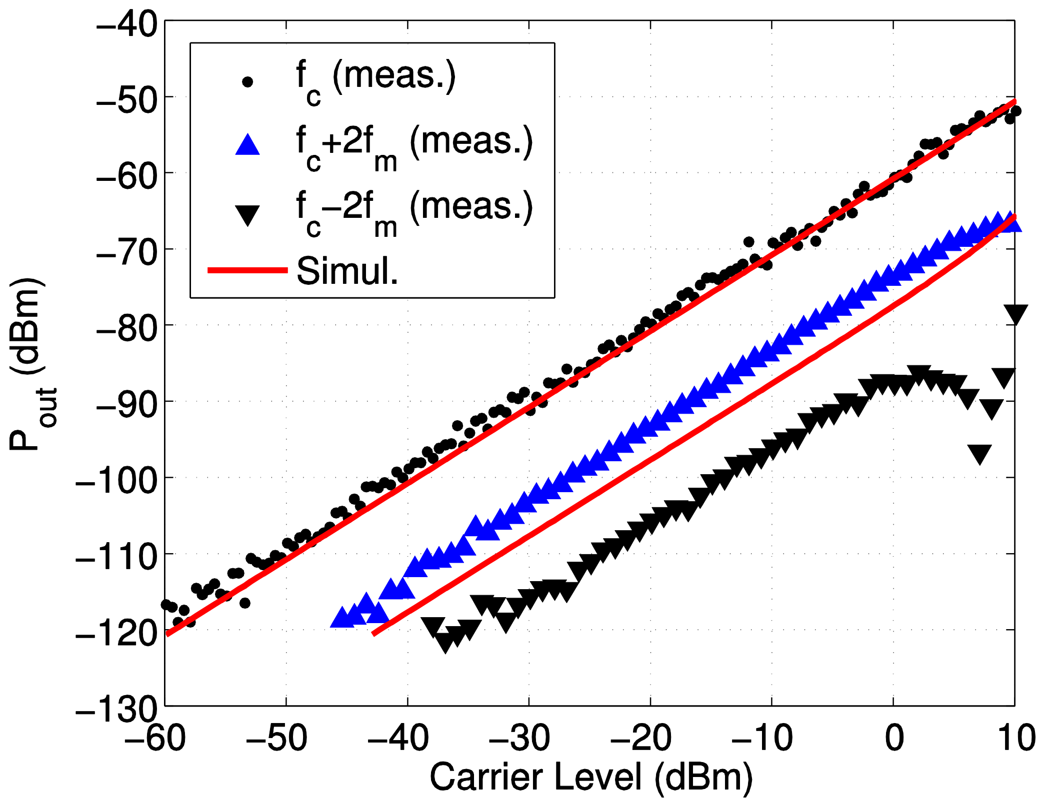

Figure 5: Level of the carrier residue and IM2 at the output of the modulator versus the carrier power. Measurements (marks) and simulation (dashed line).

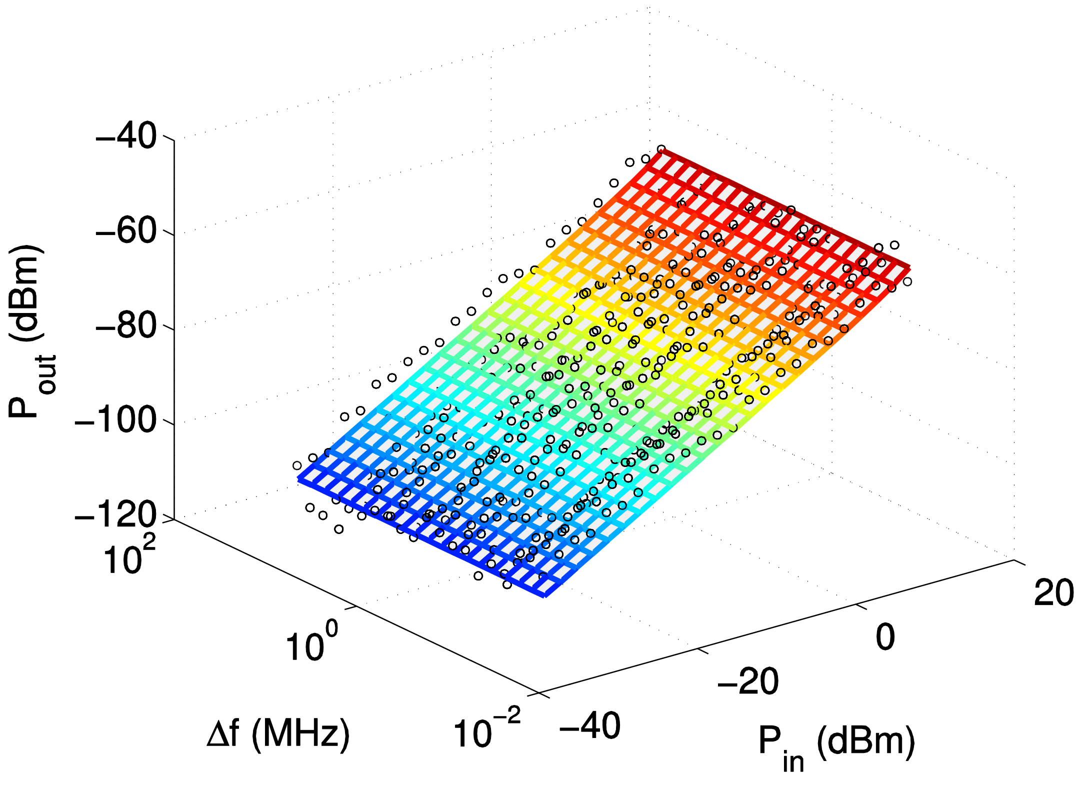

Figure 6: Level of the carrier residue versus tone spacing and carrier power. Measurements (circles) and simulation (wireframe).

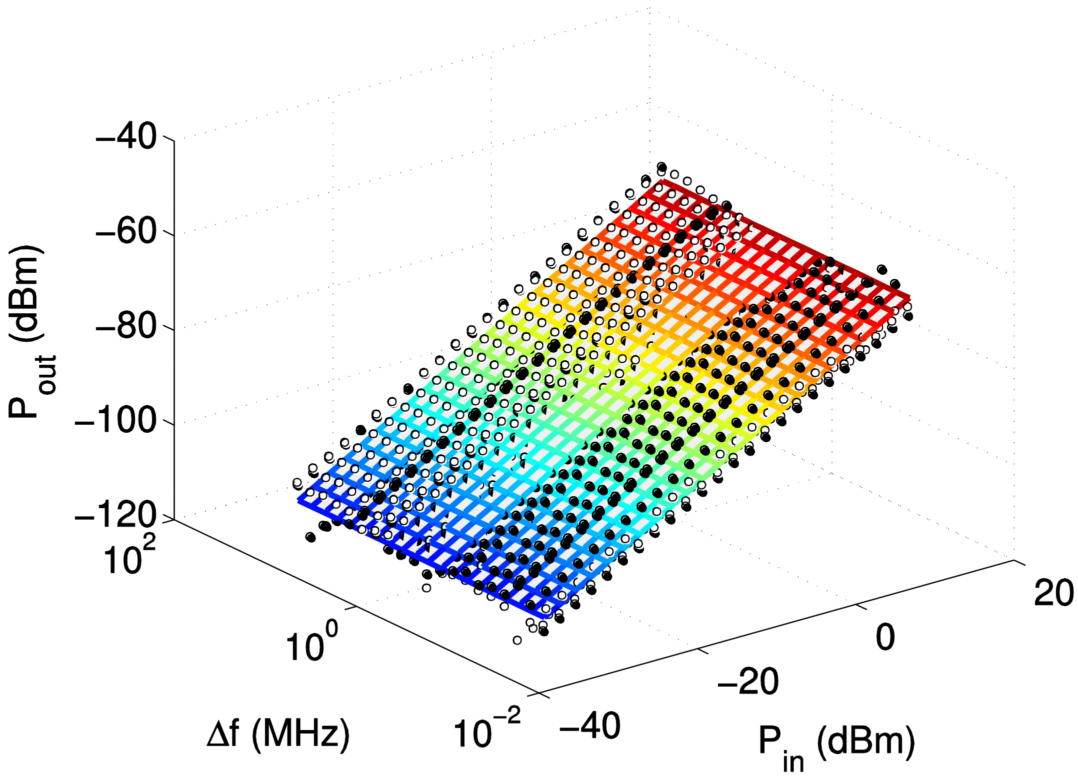

Figure 7: Level of IM2 versus tone spacing and carrier power. Measurements (black and white circles for $IM2_l$ and $IM2_u$, respectively) and simulation (wireframe).

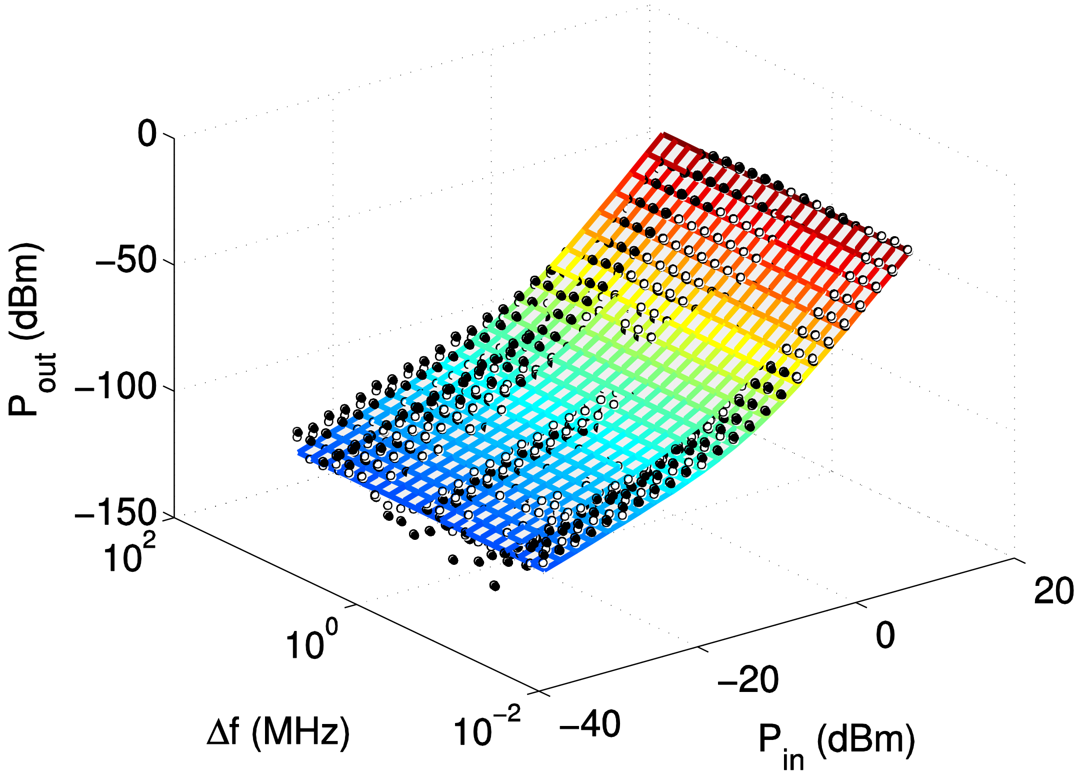

Figure 8: Level of IM3 versus tone spacing and carrier power. Measurements (black and white circles for $IM3_l$ and $IM3_u$, respectively) and simulation (wireframe).

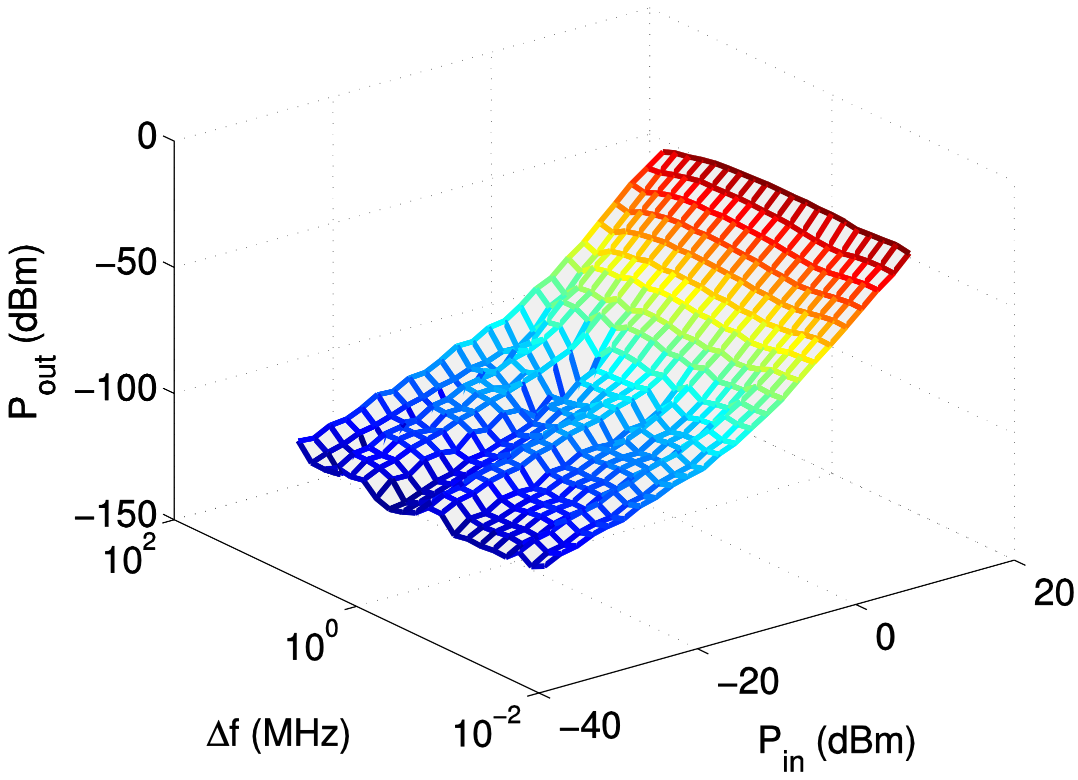

Figure 9: Measurements of the level of $IM3_u$ versus tone spacing and carrier power.